JOURNAL OF NATURAL PRODUCTS

ARTICLE

pubs.acs.org/jnp

Absolute Configuration and Selective Trypanocidal Activity of Gaudichaudianic Acid Enantiomers

João M. Batista, Jr.,*[,†] Andrea N. L. Batista,[†] Daniel Rinaldo,[†] Wagner Vilegas,[†] Daniela L. Ambrósio,[‡] Regina M. B. Cicarelli,[‡] Vanderlan S. Bolzani,[†] Massuo J. Kato,[§] Laurence A. Nafie,[⊥] Silvia N. López,[▽] and Maysa Furlan*[,†]

[†]Departamento de Química Orgânica, Instituto de Química, Universidade Estadual Paulista (UNESP), Araraquara, SP 14800-900, Brazil

[‡]Faculdade de Ciências Farmacêuticas, Universidade Estadual Paulista (UNESP), Araraquara, SP 14801-902, Brazil

[§]Instituto de Química, Universidade de São Paulo (USP), São Paulo, SP 05508-900, Brazil

[⊥]Department of Chemistry, 1-014CST, Syracuse University, Syracuse, New York 13244-4100, United States

[▽]Facultad de Ciencias Bioquímicas y Farmacéuticas, Universidad Nacional de Rosario, Suipacha 531, S2002LRK, Rosario, Argentina

Supporting Information

ABSTRACT: Gaudichaudianic acid, a prenylated chromene isolated from *Piper gaudichaudianum*, has been described as a potent trypanocidal compound against the Y-strain of *Trypanosoma cruzi*. We herein describe its isolation as a racemic mixture followed by enantiomeric resolution using chiral HPLC and determination of the absolute configuration of the enantiomers as (+)-*S* and (−)-*R* by means of a combination of electronic and vibrational circular dichroism using density functional theory calculations. Investigation of the EtOAc extract of the roots, stems, and leaves from both adult specimens and seedlings of *P. gaudichaudianum* revealed that gaudichaudianic acid is biosynthesized as a racemic mixture from the seedling stage onward. Moreover, gaudichaudianic acid was found exclusively in the roots of seedlings, while it is present in all organs of the adult plant. Trypanocidal assays indicated that the (+)-enantiomer was more active than its antipode. Interestingly, mixtures of enantiomers showed a synergistic effect, with the racemic mixture being the most active.

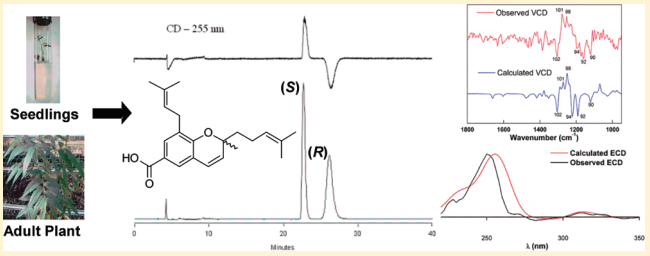

Piperaceae is a basal angiosperm family comprising more than 4000 species distributed in five genera, *Piper*, *Peperomia*, *Zippelia*, *Manekia*, and *Verhuellia*.[1] The structural richness among its members is exemplified by the large variety of secondary metabolites such as phenylpropanoids, lignan/neolignans, pyrones, aliphatic and aromatic amides, alkaloids, polyketides, benzoic acid derivatives, and benzopyrans.[2] Of these secondary metabolites, benzopyrans, represented by 2*H*-chromenes and chromanes isolated from *Piper gaudichaudianum* and *Peperomia obtusifolia*, have been demonstrated as potent trypanocidal compounds.[3,4] Of particular interest is the prenylated chromene gaudichaudianic acid (**1**), the major constituent in *P. gaudichaudianum*, which was first isolated as an enantiomerically pure metabolite[5] and showed good in vitro activity against the Y-strain of *Trypanosoma cruzi*.[3]

P. gaudichaudianum Kunth, known as pariparoba, paripaioba, muta, and jaborandi, is one of the most widely spread species in the Brazilian Atlantic Forest, from northeast to south, reaching Argentina and Paraguay.[6] The biosynthesis of the terpene moiety of its major metabolite (**1**) was shown to proceed via both the mevalonic acid and the methyl erythritol phosphate pathways.[7]

Chagas disease, also known as American trypanosomiasis, is a potentially life-threatening illness caused by the protozoan parasite *T. cruzi*. An estimated 10 million people are infected worldwide, mostly in Latin America, where Chagas disease is endemic. More than 25 million people are at risk for the disease, and it is estimated that in 2008 Chagas disease killed more than 10 000 people. During the past decades Chagas disease has been increasingly detected in the United States, Canada, and many European and some Western Pacific countries.[8]

It is well known that different stereoisomers may trigger distinct biological activities, and this feature is important in drug-like molecules.[9] On that basis, the isolation of **1** as a racemic mixture prompted us to resolve its enantiomers, determine their absolute configuration, and evaluate whether the chirality at C-2 would be critical for the biological activity. Additionally, the occurrence of a racemate, rather than an enantiomerically enriched or pure metabolite as previously reported, raised questions about the biosynthetic control of this metabolite in different plant organs or during seedling development.

Herein we describe the isolation of **1** as a racemic mixture, the resolution of its enantiomers by chiral HPLC, and the determination

Received: January 27, 2011
Published: April 20, 2011

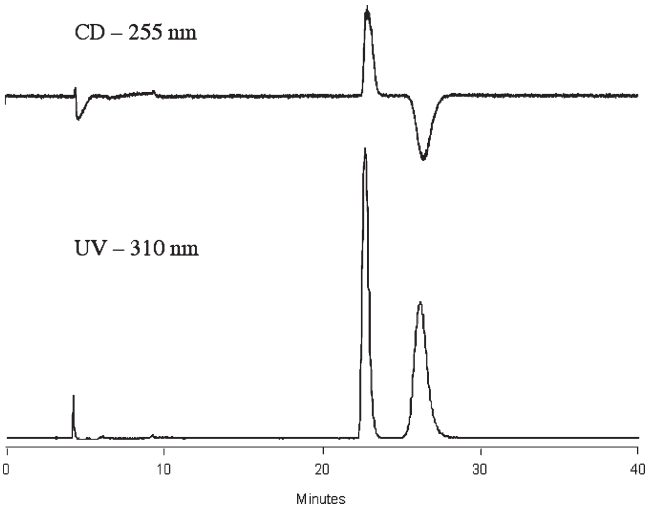

Figure 1. Chiral HPLC-PAD-CD chromatogram of racemic **1** using a Chiralcel OD-H column (250 × 4.6 mm, 5 μm); isocratic elution with *n*-hexane/EtOH (99.5:0.5, v/v), flow rate 0.7 mL/min, UV detection at 310 nm, and CD at 255 nm.

of the absolute configuration at C-2 by using a combination of electronic (ECD) and vibrational (VCD) circular dichroism associated with density functional theory (DFT) calculations. Furthermore, the evaluation of the trypanocidal potential of each enantiomer revealed a selective activity and a synergistic effect for the racemate. Finally, analyses of EtOAc extracts of different plant organs and developmental stages showed the prevalence of the racemic composition of gaudichaudianic acid.

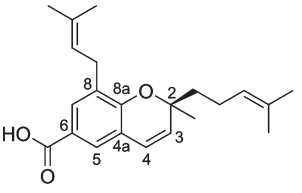

(+)-(*S*)-**1**

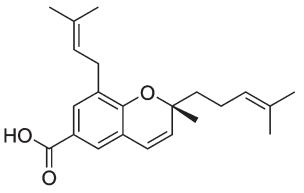

(−)-(*R*)-**1**

RESULTS AND DISCUSSION

Although gaudichaudianic acid has been routinely isolated in our research group following methodology previously described,[3,5−7] the isolation of this metabolite as a racemic mixture led us to investigate an alternative isolation protocol. On the basis of the chemical features of the 2*H*-chromene ring, the presence of protic conditions would probably have induced protonation of oxygen O-1, leading to ring-opening and formation of a phenol group as well as an allylic and tertiary carbocation. This intermediate could be attacked by the phenolic oxygen atom at either *si* or *re* faces, yielding equal proportions of *R* and *S* enantiomers (see Supporting Information). In order to eliminate this possibility, EtOAc extracts were prepared in the dark and at room temperature by maceration. No protic solvents, namely, EtOH or MeOH, or acid solution was employed throughout the isolation process. The chiral HPLC-PAD-CD chromatogram of **1**, isolated from the EtOAc extract, confirmed the presence of a racemic mixture (Figure 1).

Once the optimized chromatographic conditions for the racemic resolution of **1** were established, we proceeded with semipreparative separation of its enantiomers. After consecutive injections into the HPLC system using a Chiralcel OD-H column (250 × 10 mm, 5 μm) and flow rate of 2.5 mL/min, under the same conditions for the analytical separation, 7 mg of each enantiomer was obtained with enantiomeric excess (ee) ≥ 99%. The first peak eluted from the HPLC was determined as the (+)-enantiomer $\{[\alpha]^{25}_{D} = +21$ (c 0.36, $CHCl_3$)$\}$ followed by the (−)-enantiomer $\{[\alpha]^{25}_{D} = -21$ (c 0.36, $CHCl_3$)$\}$. It is noteworthy that the first time this metabolite was described,[5] the same specific rotation for the (+)-enantiomer was reported.

Investigation of the EtOAc extract of the roots, stems, and leaves from both adult specimens and seedlings revealed that the major metabolite (**1**) is biosynthesized as a racemic mixture. Moreover, analyses of seedling extracts showed that gaudichaudianic acid is synthesized as a racemate in the roots, while it is absent in the other plant organs (Figure 2). These findings suggest either a chemical cyclization of the geranylated benzoic acid derivative, which is the putative precursor of **1**,[7] or the presence of two enzymatic systems devoted to the formation of each enantiomer, in a similar fashion to the biosynthesis of enantiomeric monoterpenes.[10] The analysis of seedling extracts indicated that racemic **1** is found exclusively in the roots, and throughout the plant development it is also detected in the aerial organs.

After racemic resolution, the next step was the determination of the absolute configuration at C-2. As previously reported, the absolute configuration of (+)-**1** was assigned as *S* on the basis of the CD curve, which was opposite of that described for sargatriol including a positive Cotton effect at 260−280 nm (styrene chromophore). However, sargatriol has two additional stereogenic carbons in its side chain and was not appropriate as a model for direct comparison.[5,11] Chiroptical properties such as ECD and VCD have gained increased attention in recent years. The increasing interest in these methods is due to the reliability of their applications to chiral molecular structure determination and the ease with which they can be measured and calculated with recent advances in quantum-chemical methods.[12] The circular dichroism phenomenon arises from the differential absorption for left and right circularly polarized light by a chiral molecule, ECD being the most widely practiced. VCD is an extension of ECD into infrared and near-infrared regions of the spectrum, where vibrational transitions occur within the ground electronic state of the molecule.[13] Recently, the combination of ECD, VCD, and quantum-mechanical calculations was used to reassign the absolute configuration of a related benzopyran,[14] which had had its absolute configuration determined on the basis of ECD empirical helicity rules,[15] similar to the sargatriol case.[16] The possibility of exceptions in the interpretation of ECD relying on empirical rules led us to simulate both ECD [B3LYP/6-311++G(2d,2p)//B3LYP/6-31G(d)] and VCD [B3LYP/6-31G(d)] spectra of **1** using time-dependent density functional theory (TDDFT) and DFT calculations, respectively. The ECD curve obtained for the Boltzmann-averaged eight lowest-energy conformers of **1**, all of which presented the bulky prenyl chain in the pseudoequatorial position (Figure 3), and that for the experimental (+)-**1** were similar, but not fully opposite that of sargatriol. Interestingly, the measured and calculated Cotton effects at 260−290 nm (^1L_b band) were negative for *M*-helicity of the chromene ring (Figure 4), in what may constitute another exception to Crabbé's "inverse" styrene helicity rule.[17] In spite of slight differences between the

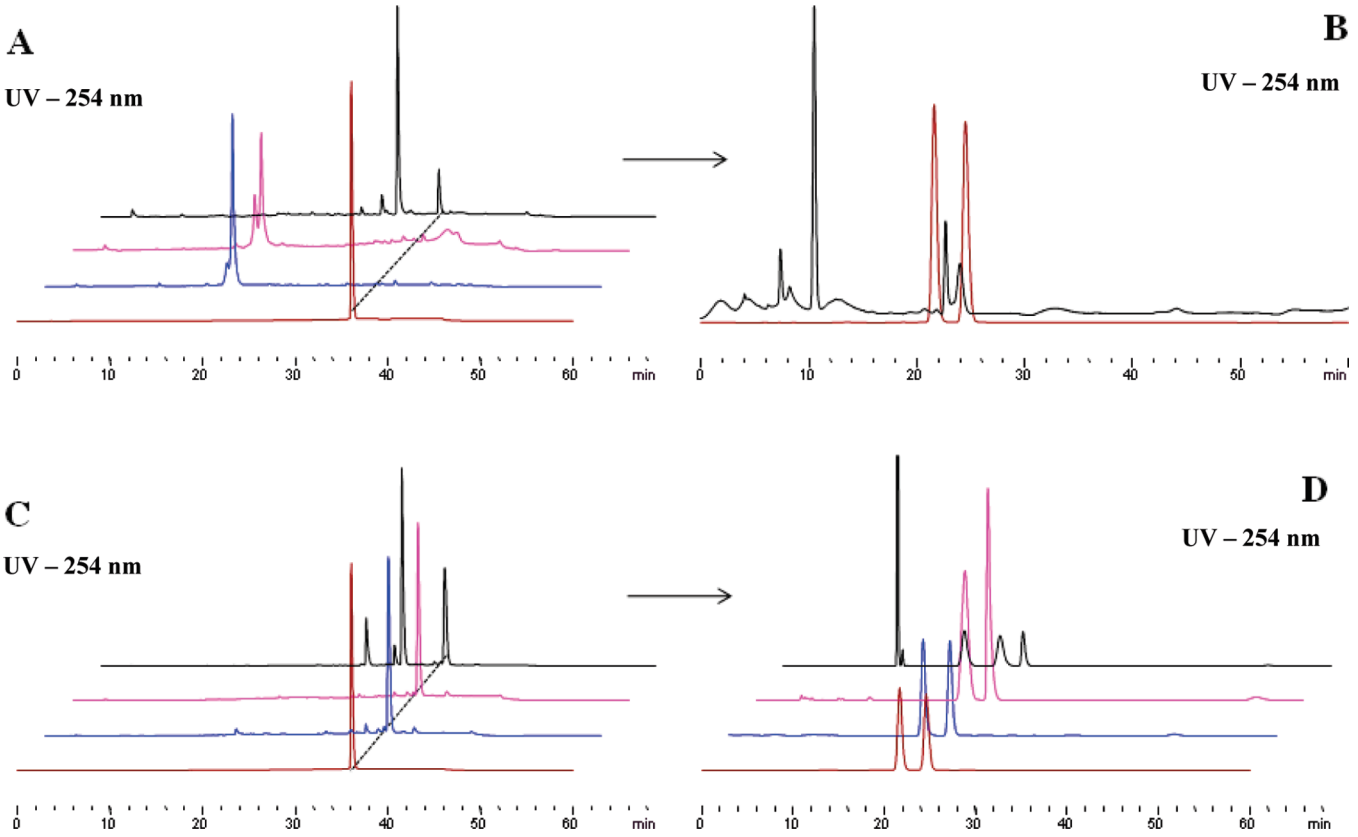

Figure 2. HPLC-PAD chromatograms of racemic **1** (brown) and EtOAc extracts of leaves (blue), stems (pink), and roots (black). Upper frame: seedling chromatograms (A) C-18 and (B) chiral. Lower frame: adult plant chromatograms (C) C-18 and (D) chiral. Conditions: (A and C) Phenomenex Luna C-18 (250 × 4.6 mm, 5 μm), linear gradient of 0.05% aqueous HOAc and MeOH, 5−95% MeOH in 30 min, and then 10 min 100% MeOH, 1.0 mL/min; (B and D) Phenomenex LUX Cellulose-1 (250 × 4.6 mm, 5 μm), isocratic elution with *n*-hexane/EtOH (99.5:0.5) + 0.05% HOAc, 0.8 mL/min.

previously described ECD spectrum and the one reported herein, the absolute configuration of (+)-**1** was confirmed as *S*, and consequently (−)-**1** was assigned an *R* absolute configuration.

In order to gain more confidence about the absolute configurations assigned for the enantiomers of **1**, VCD calculations and measurements were carried out. Although only a small amount of each enantiomer was available, approximately 1.5 mg, the major features of the VCD spectrum were observed above the noise level and confirmed the absolute configuration of (+)-**1** as *S* and (−)-**1** as *R* (Figure 5). For both ECD and VCD calculations, the same eight lowest-lying conformers obtained after geometry optimization using the B3LYP/6-31G(d) level of theory were considered for further calculations. IR and VCD frequency calculations at the B3LYP/6-31G(d) level of theory resulted in no imaginary frequencies, confirming the considered conformers as real minima. Due to the presence of a flexible prenyl chain linked to the stereogenic center and the possibility of ring puckering, the initial steps of conformational search and geometry optimization were carried out for a fragment molecule (Figure 5). The lowest-energy fragment conformers were used to construct the complete molecule of **1**. Beyond this point, conformational searches and geometry optimizations were carried out with the preoptimized cores constrained. As a great number of conformers were found, we calculated IR and VCD spectra for the Boltzmann-averaged four lowest-energy conformers of the fragment molecule and evaluated whether it would contain enough structural information for an unambiguous assignment of the absolute configuration. Indeed, comparison of the calculated IR and VCD spectra of the (*S*)-fragment with those calculated for (*S*)-**1** revealed the presence of three important VCD bands at 1190, 1250, and 1310 cm^{-1}, which can be used to unambiguously assign the absolute configuration of the C-2 stereogenic center (Figure 5). It is also noteworthy that for both the fragment and the whole molecule **1** all IR and VCD calculations were carried out considering these molecules as dimers (hydrogen bonded to formic acid to simulate a carboxylic acid dimer at the molecule−molecule interface). This procedure is considered to provide better agreement between experimental and calculated VCD data when gas phase calculations and measurements in apolar solvents are used.[14,18] Nevertheless, no dimer linkage was considered for ECD calculations in order to avoid the presence of extra electronic transitions arising from the additional carboxyl group of the formic acid used in the dimer simulation.

Following the racemic resolution and the determination of the absolute configuration of each enantiomer, the next step was the evaluation of the trypanocidal activity of the single enantiomers. Initially, pure enantiomers and the racemic mixture were evaluated against the Y-strain of *T. cruzi* epimastigote forms. Surprisingly, the racemic mixture showed the most potent activity (IC_{50} 55.8 ± 2.2 μM) followed by (+)-(*S*)-**1** (IC_{50} 176.5 ± 2.0 μM) and (−)-(*R*)-**1** (IC_{50} 223.5 ± 2.5 μM). These results led us to investigate a possible synergistic effect since the 50:50

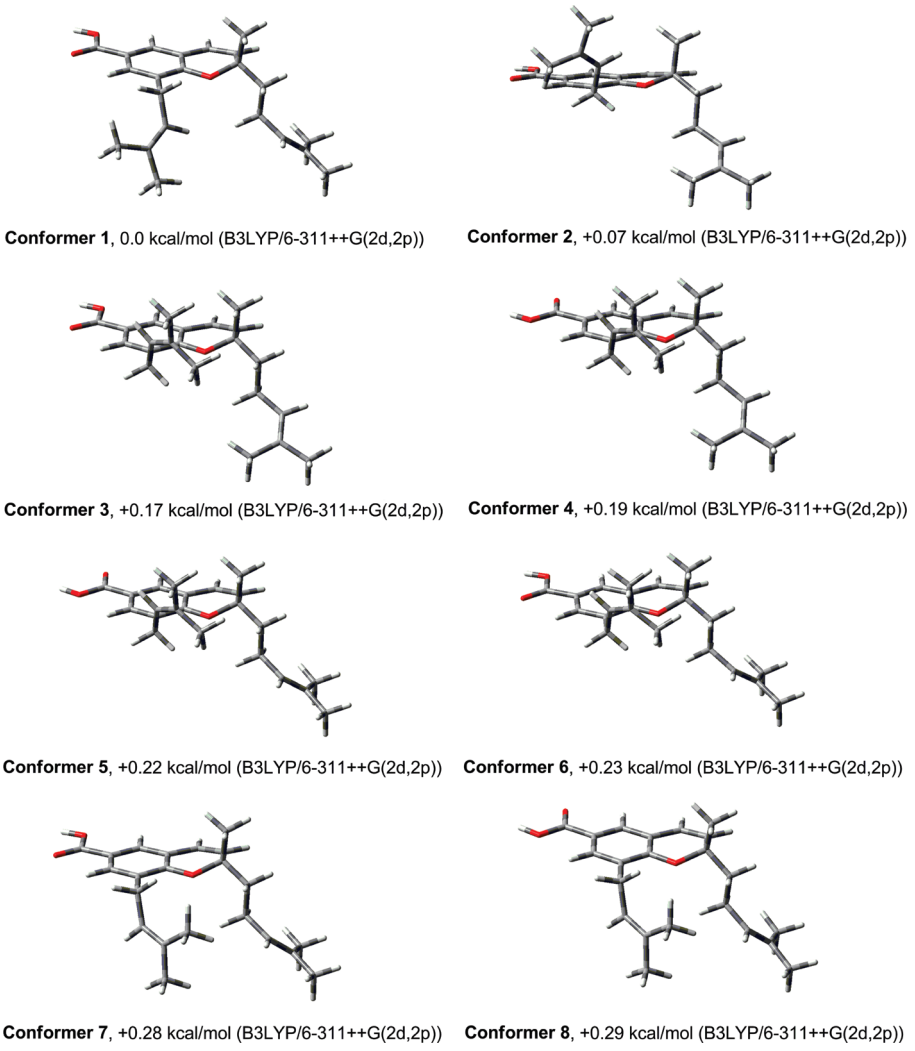

Figure 3. Structure and relative energy of the eight lowest-energy conformers of (*S*)-**1** used for ECD calculations at the B3LYP/6-311++G(2d,2p) level of theory.

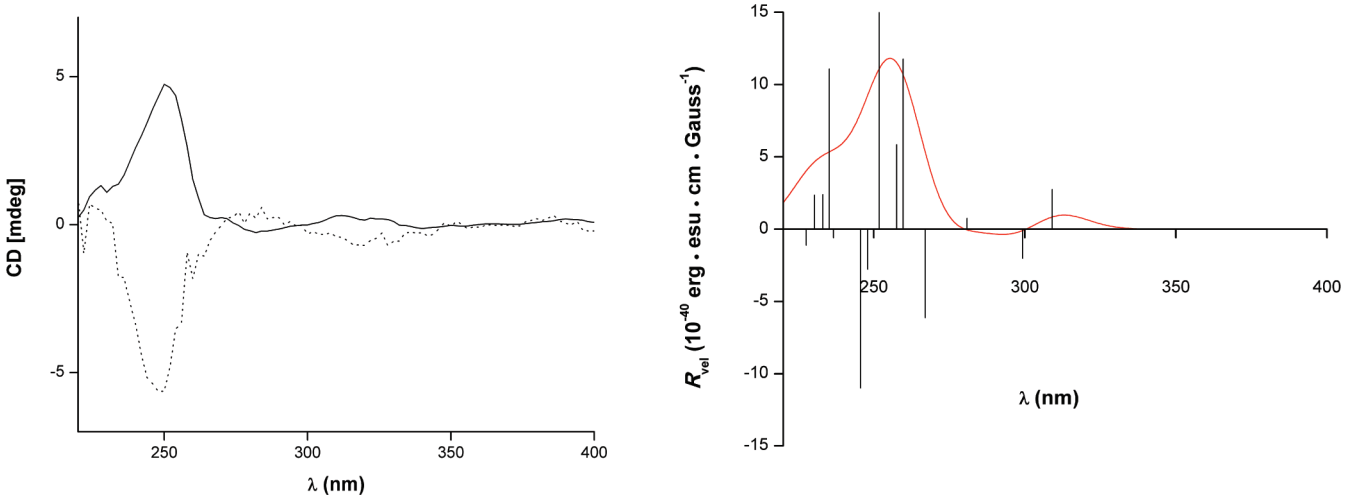

Figure 4. (Left) Experimental ECD spectra of the enantiomers of **1** assigned as (+)-*S* (solid line) and (−)-*R* (dotted line). (Right) Calculated ECD spectra [B3LYP/6-311++G(2d,2p)//B3LYP/6-31G(d)] of the Boltzmann average of the eight lowest-energy conformers of the corresponding (*S*)-**1**. The bars represent the rotational strengths for the weighted ECD spectrum.

dx.doi.org/10.1021/np200085h |*J. Nat. Prod.* 2011, 74, 1154–1160

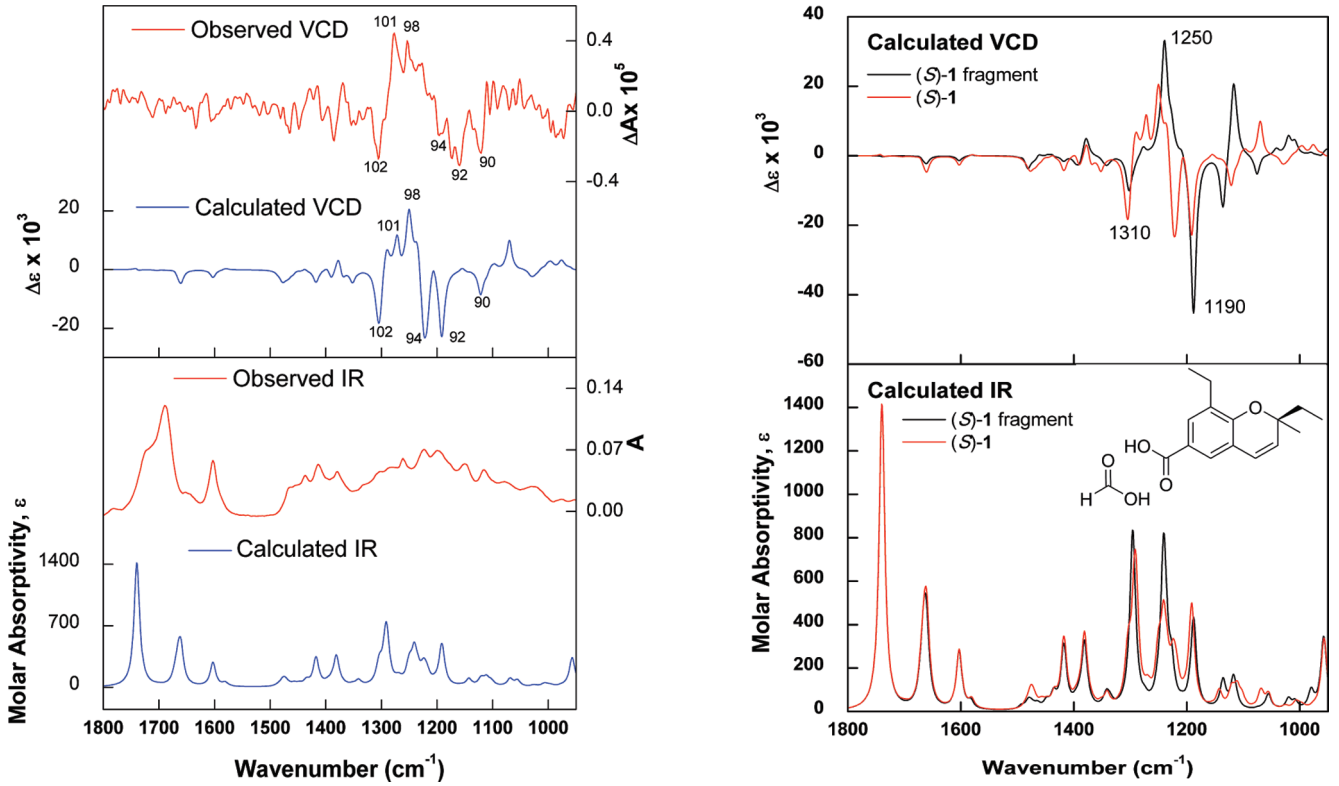

Figure 5. (Left) Comparison of the VCD and IR spectra of measured (+)-**1** with calculated [B3LYP/6-31G(d)] VCD and IR spectra of the Boltzmann average of the eight lowest-energy conformers of the corresponding (*S*)-**1**. The comparison establishes the absolute configuration of this molecule as (+)-(*S*)-**1**. Numbers represent selected fundamentals. (Right) Comparison of the VCD and IR spectra [B3LYP/6-31G(d)] of the calculated (*S*)-**1** fragment and the whole molecule (*S*)-**1**. Numbers represent selected vibrational frequencies.

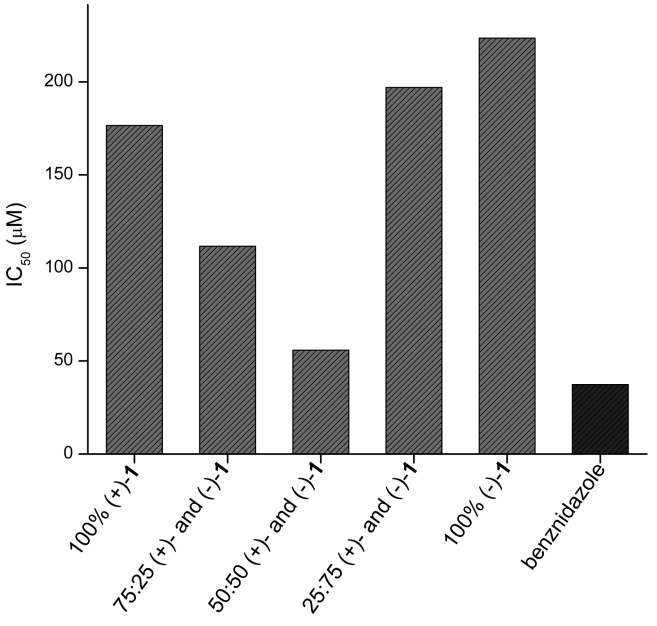

Figure 6. Trypanocidal activity of the enantiomers of **1** in several proportions. Benznidazole was used as positive control.

mixture of (+)- and (−)-**1** was more active than each enantiomer separately. Additionally, mixtures of 75:25 (IC_{50} 111.2 ± 4.3 μM) and 25:75 (IC_{50} 197.0 ± 1.4 μM) of (+)- and (−)-**1** were also assayed. The results of the trypanocidal activity are presented in Figure 6.

According to the data presented (Figure 6), there really is a synergistic effect regarding enantiomers of **1**, with the (+)-(*S*)-enantiomer playing the most important role. However, the maximum trypanocidal activity is achieved only when both enantiomers are present in equal proportions with activity comparable to that of the positive control benznidazole (IC_{50} 37.3 ± 1.5 μM). In proportions other than the maximum one, the best activities are directly proportional to the percentage of (+)-(*S*)-**1**. This is the first time a synergistic effect of enantiomers of a bioactive natural product is reported against *T. cruzi*. Finally, the finding of the racemic mixture of **1** with trypanocidal activity comparable to that of the positive control benznidazole suggests that in our previous work dealing with trypanocidal activity of gaudichaudianic acid we had indeed a racemic mixture instead of the *S* enantiomer as reported.[3]

In conclusion, in this work we achieved the isolation of gaudichaudianic acid as a racemic mixture, its resolution using chiral chromatography, and the determination of the absolute configuration of the enantiomers as (+)-(*S*)-**1** and (−)-(*R*)-**1** using a combination of ECD, VCD, and DFT calculations. The absolute configuration assigned to (+)-(*S*)-**1** was in accordance with a previous report. Additionally, chiral HPLC-PAD analyses of EtOAc extract of roots, stems, and leaves from both adult specimens and seedlings revealed that this metabolite is biosynthesized as a racemic mixture from its initial developmental stages onward. Trypanocidal assays carried out for both enantiomers indicated the (+)-enantiomer to be more active than its antipode.

Interestingly, mixtures of both enantiomers in several proportions pointed out a synergistic effect with maximum relative activity achieved for the 50:50 mixture.

EXPERIMENTAL SECTION

General Experimental Procedures. NMR spectra were obtained with a Varian INOVA NMR spectrometer at 500 MHz for ^{1}H and 125 Hz for ^{13}C using TMS as chemical shift reference. The HRESIMS spectra were obtained on a Bruker ultrOTOF-Q-ESI-TOF mass spectrometer. Silica gel 60 (Merck, 0.063−0.200 mm) and C-18 were used in column chromatographic separations. HPLC separations were performed on a Shimadzu LC-6AD equipped with an SPD-M20A photodiode array detector or on a Jasco 2000 HPLC equipped with a PU-2089 Plus pump, an MD-2010 Plus photodiode array detector, and a CD-2095 Plus circular dichroism detector. Chiralcel OD-H (250 × 4.6 mm and 250 × 10 mm, 5 μm) as well as Phenomenex Lux Cellulose-1 (250 × 4.6 mm, 5 μm) chiral columns were used. All solvents were of HPLC or analytical grade. The IR and VCD spectra were recorded with a modified BioTools Dual-PEM ChiralIR FT-VCD spectrometer using a resolution of 4 cm^{-1} and a collection time of 11 h. The optimum retardation of the two ZnSe photoelastic modulators (PEMs) was set at 1400 cm^{-1}. An optical band-pass filter was used to allow only the spectral region 800−2000 cm^{-1} to reach the detector. Spectra were calibrated automatically, using the standard calibration files. VCD spectra were recorded in $CDCl_3$ solution (1.5 mg of each compound in 100 μL of $CDCl_3$ in a BaF_2 cell with 100 μm path length). Baseline offsets were eliminated by subtracting the VCD spectra of the enantiomer and its antipode and dividing by 2. Optical rotations at 589 nm were recorded in $CHCl_3$ on a Perkin-Elmer 241 polarimeter, at 25 °C, using a 10 cm cell. The ECD spectra of each enantiomer eluting from the chiral HPLC were measured in the Jasco CD-2095 detector by trapping in a 1.0 cm quartz cell through a switching valve. The spectra were average computed over three instrumental scans, and the intensities are presented in terms of ellipticity values (mdeg). The ECD spectra were corrected by baseline subtraction obtained from a measurement of the same solvent used (*n*-hexane/EtOH, 99.5:0.5).

Plant Material. Leaves, stems, and roots from an adult specimen of *P. gaudichaudianum* Kunth were collected on the campus of the Universidade de São Paulo (Brazil) and were identified by Dr. Elsie F. Guimarães. A voucher specimen (Kato-0093) was deposited at the Herbarium of the Instituto de Botânica, São Paulo, Brazil. Seedlings were grown from seeds of *P. gaudichaudianum*, sown in Murashige and Skoog basic nutrient medium,[19] for nine weeks. After this period, the seedlings were transferred to soil-filled plastic pots, from where they were harvested after six weeks.

Extraction and Isolation. For the qualitative analysis of extracts, powdered leaves, stems, and roots from an adult plant were extracted with EtOAc in the dark at room temperature for 3 h. The solvent was evaporated under reduced pressure without heating, and the samples were promptly injected into the HPLC system for both reversed-phase and chiral evaluation. The seedlings were harvested, and each individual organ was immediately triturated in liquid N_2 followed by extraction with EtOAc in the dark at room temperature for 3 h. The solvent was evaporated under reduced pressure without heating, and the samples were promptly injected into the HPLC system for the same analyses.

Gaudichaudianic acid (**1**) was isolated from the EtOAc extract of leaves from an adult specimen. Powdered, air-dried leaves (500 g) were extracted by maceration with EtOAc (5 × 2 L) at room temperature. The resulting solution was concentrated under reduced pressure to yield 17 g of crude extract, which was subjected to CC over silica gel (20 × 8 cm), using gradient elution from hexanes to EtOAc and from EtOAc to MeOH, affording 50 fractions. Fractions 17 and 18 were pooled and then subjected to low-pressure column chromatography over silica C-18 (12 × 3 cm) under gradient elution of 80% to 100% MeOH in H_2O, yielding seven fractions. Gaudichaudianic acid (200 mg) was obtained from fraction 3. Identification of racemic **1** and its enantiomers was supported by spectroscopic analysis including NMR spectroscopy and HRESIMS (see Supporting Information) in comparison with published data.[5]

Biological Assay. In vitro trypanocidal assays were performed in triplicate with epimastigote forms of *T. cruzi* Y-strain, which were grown axenically at 28 °C in liver-infusion tryptose (LIT) medium supplemented with 10% fetal calf serum and harvested during exponential phase of growth (7-day-old culture forms). Single enantiomers and mixtures were dissolved in DMSO and further added to a 96-well tissue culture plate in different final concentrations (100, 50, 25, 10, 5, 2.5, and 1 μg/mL). *T. cruzi* (1 × 10^7 parasites/mL) was added to each test well, and the same volume of LIT medium (50 μL), with and without parasites, was added into the control wells without test compounds. These plates were maintained at 28 °C for 72 h. After this period, a 10 μL aliquot of 2.5 mg/mL 3-(4,5-dimethylthiazol-2-yl)-2,5-diphenyltetrazolium bromide−phenazinemethosulfate (MTT−PMS) solution was added to each well, and the plates were incubated for 75 min in the dark at 28 °C. Subsequently, a solution of 10% (100 μL) sodium dodecyl sulfate was added to each well and maintained at room temperature in the dark for 30 min. Absorbance of the samples was read at 595 nm. The 50% inhibitory concentration (IC_{50}) values of the test compounds and positive control benznidazole were determined by calculating the percentage of cytotoxicity.[20,21]

Computational Methods. All DFT and TDDFT calculations were carried out at 298 K in the gas phase with Gaussian 03 and/or 09.[22] Calculations were performed for arbitrarily chosen (*S*)-**1**, the enantiomer first described.[5] The first steps of conformational search and geometry optimization were carried out for a fragment molecule (see Supporting Information). All conformational searches were carried out at the molecular mechanics level of theory employing MM+ and MMFF force fields incorporated in Hyperchem 7 and Spartan 08 software packages, respectively. For the fragment of compound **1**, 32 conformers with relative energy (E_{rel}) within 6 kcal/mol of the lowest-energy conformer were selected and further geometry optimized at the B3LYP/6-31G(d) level of theory. Of these, 13 conformers (Boltzmann distribution ≥2%) were selected to build up the whole molecule **1**. After adding the prenyl groups, a new conformational search was carried out at the molecular mechanics level of theory; however, the preoptimized cores were constrained. As a result, 70 conformers (E_{rel} ≤ 3 kcal/mol) were found and geometry optimized at the B3LYP/6-31G(d) level of theory. Among 19 conformers with E_{rel} ≤ 1.0 kcal/mol, the eight lowest-energy conformers were considered for ECD spectral calculation. TDDFT was employed to calculate excitation energy (in nm) and rotatory strength *R* in dipole velocity (R_{vel} in cgs units: 10^{-40} erg esu cm G^{-1}) form, at the B3LYP/6-311++G(2d,2p) level of theory. The calculated rotatory strengths from the first 14 singlet → singlet electronic transitions were simulated into an ECD curve using Gaussian band shapes and 15 nm half-width at 1/*e* of peak height. The predicted wavelength transitions are used as such without any scaling. IR and VCD spectra were calculated for the same eight lowest-energy conformers, but this time as dimers with formic acid. Dipole and rotational strengths from Gaussian were converted into molar absorptivities (M^{-1} cm^{-1}), and each spectrum was plotted as a sum of Lorentzian bands with half-widths of 6 cm^{-1}. The calculated wavenumbers were multiplied with a scaling factor of 0.97, and the Boltzmann-population-weighted composite spectra were plotted using Origin software. The adequacy of B3LYP/6-31G(d) for the optimization of geometry and calculation of IR and VCD spectra as well as B3LYP/6-311++G(2d,2p) for ECD calculations has been previously demonstrated.[14]

■ ASSOCIATED CONTENT

Supporting Information. Acid-mediated ring-opening mechanism of **1**. Lowest-energy conformers of (*S*)-**1** and fragment as dimers with formic acid; VCD and ECD spectra of individual conformers; molecular orbitals involved in key ECD transitions of (*S*)-**1**; ^{1}H NMR spectra of **1**; HRESIMS spectrum of **1**. This material is available free of charge via the Internet at http://pubs.acs.org.

■ AUTHOR INFORMATION

Corresponding Author

*Tel: +55-16-3301-9661. Fax: +55-16-3301-9692. E-mail: maysaf@reitoria.unesp.br (M.F.); joaombj@hotmail.com (J.B.).

■ ACKNOWLEDGMENT

The authors thank BioTools, Inc. for the use of its computational facility. This work was supported with grants provided by the State of São Paulo Research Foundation (FAPESP) within the BIOTA/FAPESP—Biodiversity Virtual Institute Program (www.biotasp.org.br) (2003/02176-7). J.M.B.J. thanks FAPESP for the provision of a scholarship (2008/58658-3) and The Brazilian Federal Agency for Support and Evaluation of Graduate Education (CAPES), within the PDEE program (3686/09-4), for the international scholarship. S.N.L. thanks CONICET and FONCYT. W.V., V.S.B., M.J.K., and M.F. are also grateful to the National Council for Scientific and Technological Development (CNPq) for research fellowships.

■ REFERENCES

(1) Samain, M. S.; Vrijdaghs, A.; Hesse, M.; Goetghebeur, P.; Rodríguez, F. J.; Stoll, A.; Neinhuis, C.; Wanke, S. *Ann. Bot.* **2010**, *105*, 677–688.

(2) López, S. N.; Lopes, A. A.; Batista, J. M., Jr.; Flausino, O., Jr.; Bolzani, V. S.; Kato, M. J.; Furlan, M. *Biores. Technol.* **2010**, *101*, 4251–4260.

(3) Batista, J. M., Jr.; Lopes, A. A.; Ambrósio, D. L.; Regasini, L. O.; Kato, M. J.; Bolzani, V. S.; Cicarelli, R. M. B.; Furlan, M. *Biol. Pharm. Bull.* **2008**, *31*, 538–540.

(4) Mota, J. S.; Leite, A. C.; Batista Junior, J. M.; López, S. N.; Ambrósio, D. L.; Passerini, G. D.; Kato, M. J.; Bolzani, V. S.; Cicarelli, R. M. B.; Furlan, M. *Planta Med.* **2009**, *75*, 620–623.

(5) Lago, J. H. G.; Ramos, C. S.; Casanova, D. C. C.; Morandim, A. A.; Bergamo, D. C. B.; Cavalheiro, A. J.; Bolzani, V.; da, S.; Furlan, M.; Guimarães, E. F.; Young, M. C. M.; Kato, M. J. *J. Nat. Prod.* **2004**, *67*, 1783–1788.

(6) Ramos, C. S.; Vanin, S. A.; Kato, M. J. *Chemoecology* **2009**, *19*, 73–80.

(7) Lopes, A. A.; Baldoqui, D. C.; López, S. N.; Kato, M. J.; Bolzani, V. S.; Furlan, M. *Phytochemistry* **2007**, *68*, 2053–2058.

(8) World Health Organization (WHO): Fact sheet No. 340, June 2010, Chagas Disease (American Trypanosomiasis). Available at http://www.who.int/mediacentre/factsheets/fs340/en/index.html. Accessed December 1, 2010.

(9) Kuppens, T.; Bultinck, P.; Langenaeker, W. *Drug Discovery Today Technol.* **2004**, *1*, 269–275.

(10) Dewick, P. M. *Medicinal Natural Products—A Biosynthetic Approach*, 3rd ed.; John Wiley & Sons: West Sussex, 2009; p 198.

(11) Velozo, L. S. M.; Ferreira, M J. P.; Santos, M. I. S.; Moreira, D. L.; Emerenciano, V. P.; Kaplan, M. A. C. *Phytochemistry* **2006**, *67*, 492–496.

(12) Polavarapu, P. L.; Scalmani, G.; Hawkins, E. K.; Rizzo, C.; Jeirath, N.; Ibnusaud, I.; Habel, D.; Nair, D. S.; Haleema, S. *J. Nat. Prod.* **2011**, *3*, 321−328.

(13) Freedman, T. B.; Cao, X.; Dukor, R. K.; Nafie, L. A. *Chirality* **2003**, *15*, 743–758.

(14) Batista, J. M., Jr.; Batista, A. N. L.; Rinaldo, D.; Vilegas, W.; Cass, Q. B.; Bolzani, V. S.; Kato, M. J.; López, S. N.; Furlan, M.; Nafie, L. A. *Tetrahedron: Asymmetry* **2010**, *21*, 2402–2407.

(15) Batista, J. M., Jr.; López, S. N.; Mota, J. S.; Vanzolini, K. L.; Cass, Q. B.; Rinaldo, D.; Vilegas, W.; Bolzani, V. S.; Kato, M. J.; Furlan, M. *Chirality* **2009**, *21*, 799–801.

(16) Kikuchi, T.; Mori, Y.; Yokoi, T.; Nakazawa, S.; Kuroda, H.; Masada, Y.; Kitamura, K.; Kuriyama, K. *Chem. Pharm. Bull.* **1983**, *31*, 106–113.

(17) Kwit, M.; Gawronski, J.; Boyd, D. R.; Sharma, N. D.; Kaik, M.; O_Ferrall, R. A. M.; Kudavalli, J. S. *Chem.—Eur. J.* **2008**, *14* 11500–11511.

(18) Freedman, T. B.; Cao, X.; Phillips, L. M.; Cheng, P. T. W.; Dalterio, R.; Shu, Y. Z.; Zhang, H.; Zhao, N.; Shukla, R. B.; Tymiak, A.; Gozo, S. K.; Nafie, L. A.; Gougoutas, J. Z. *Chirality* **2006**, *18*, 746–753.

(19) Murashige, T.; Skoog, F. *Plant Physiol.* **1962**, *15*, 473–497.

(20) Muelas-Serrano, S.; Nogal-Ruiz, J. J.; Gómez-Barrio, A. *Parasitol. Res.* **2000**, *86*, 999–1002.

(21) Cotinguiba, F.; Regasini, L. O.; Bolzani, V. S.; Debonsi, H. M.; Passerini, G. D.; Cicarelli, R. M. B.; Kato, M. J.; Furlan, M. *Med. Chem. Res.* **2009**, *18*, 703–711.

(22) Frisch, M. J.; Trucks, G. W.; Schlegel, H. B.; Scuseria, G. E.; Robb, M. A.; Cheeseman, J. R.; Scalmani, G.; Barone, V.; Mennucci, B.; Petersson, G. A.; Nakatsuji, H.; Caricato, M.; Li, X.; Hratchian, H. P.; Izmaylov, A. F.; Bloino, J.; Zheng, G.; Sonnenberg, J. L.; Hada, M.; Ehara, M.; Toyota, K.; Fukuda, R.; Hasegawa, J.; Ishida, M.; Nakajima, T.; Honda, Y.; Kitao, O.; Nakai, H.; Vreven, T.; Montgomery, J. A., Jr.; Peralta, J. E.; Ogliaro, F.; Bearpark, M.; Heyd, J. J.; Brothers, E.; Kudin, K. N.; Staroverov, V. N.; Kobayashi, R.; Normand, J.; Raghavachari, K.; Rendell, A.; Burant, J. C.; Iyengar, S. S.; Tomasi, J.; Cossi, M.; Rega, N.; Millam, J. M.; Klene, M.; Knox, J. E.; Cross, J. B.; Bakken, V.; Adamo, C.; Jaramillo, J.; Gomperts, R.; Stratmann, R. E.; Yazyev, O.; Austin, A. J.; Cammi, R.; Pomelli, C.; Ochterski, J. W.; Martin, R. L.; Morokuma, K.; Zakrzewski, V. G.; Voth, G. A.; Salvador, P.; Dannenberg, J. J.; Dapprich, S.; Daniels, A. D.; Farkas, O.; Foresman, J. B.; Ortiz, J. V.; Cioslowski, J.; and D. J. Fox. *Gaussian 09*, Revision A.02; Gaussian, Inc.: Wallingford, CT, 2009.